3 Materials, Methodology and Characterization Techniques

3.1 Overview

This chapter covers the experimental details involved in the synthesis of the materials used in this research, as well as the fundamentals of experimental methods and protocols. However, each chapter has a different theme. Basic materials and techniques used in each chapter will be defined throughout this chapter.

3.1 Materials and Method

This section provides the details about the materials used in this work including where they were obtained from and what precursors were used in this work. This section also gives details about their synthesis procedures.

3.2.1 Zirconia substituted 1393 bioactive glass preparation

The synthesis of bioactive glass nanoparticles followed the sequence of sol preparation, drying, and sintering. The weight of precursors used for each composition was determined by iterating the weight of the precursor with its respective molar weight across the different precursors used, to obtain the moles of each precursor for the desired glass composition. The Zirconia substituted 1393 bioactive glass used throughout this work was made via sol-gel method using high purity Tetraethyl orthosilicate (TEOS; with chemical formula $Si(OC_2H_5)_4$, purchased from Sigma Aldrich, ≥ 99% purity), TEP (Triethyl phosphate, Sigma Aldrich ≥ 98% purity), Calcium nitrate tetrahydrate ($(Ca(NO_3)_2 \cdot 4H_2O$, Sigma Aldrich, ≥ 99% purity), Magnesium nitrate hexahydrate (Loba Chemicals, ≥ 99% purity), Sodium nitrate (Loba Chemicals, ≥ 98% purity), Potassium nitrate (Loba Chemicals, ≥ 98% purity), and Zirconium oxynitrate hydrate ($ZrO(NO_3)_2.xH_2O$, Sigma Aldrich, ≥ 99% purity), and 69% HNO_3 solution (Sigma Aldrich). The glass used within this work is stated in mol% in **Table 3.1**.

Table 3.1 Chemistry of the glass used within this work in mol%

Oxide	SiO_2	CaO	Na_2O	P_2O_5	K_2O	MgO	ZrO_2
Mol%	53.10	22.10	6.00	1.70	7.90	7.7	1.50

To prepare 5 gm of substituted bioglass, firstly required amount of TEOS was added into 20 ml of 0.1 N HNO_3 solutions and stirred for 45 min to complete the hydrolysis reaction. TEP, Calcium nitrate tetrahydrate, Magnesium nitrate hexahydrate, Sodium nitrate, Potassium nitrate, and Zirconium oxynitrate hydrate were added in the required amount and stirred for 45 min individually to obtain a transparent sol. Sol was aged at room temperature for hydrolysis and polycondensation reaction until gel formation takes place. The gel was dried at 60°C for 24hr. The dried gel was thermally treated at 600°C to obtain the amorphous nature of glass.

3.2.1.1 Drying

Drying is an important stage in the processing of bioactive glass nanoparticles for the control of nanoparticle morphology (specific surface area, pore size, shape, and volume). The bioactive glass nanoparticles obtained from the sol-gel route were subjected to an oven drying process. Oven drying is a common method of air drying the gels in an open container, accelerated through heating the materials in an oven (Zhong et al., 2000). In this study, the bioactive glass was placed in a drying oven with a temperature maintained at 60°C for 24 h.

3.2.1.2 Sintering

Sintering is the next stage in the processing of bioactive glass to ensure the incorporation of calcium into the silicate network and the removal of nitrate and other impurities (Labbaf et al., 2011). Once the drying step was completed, the bioactive glass nanoparticles were removed from their respective environments and heat-treated in inert

alumina crucibles in the oven. The products were heat-treated to 600°C using a holding time of 6 h, with a heating and cooling rate of 2°C/min from room temperature.

3.2.2 Hydroxyapatite bioceramic preparation

In the wet-chemical process, hydroxyapatite (HA) is precipitated via mixing the aqueous solutions of compounds containing Ca and P ions. $CaCl_2$, $Ca(NO_3)_2$, $Ca(OH)_2$, $CaCO_3$, $CaSO_4.2H_2O$, and $(CH_3COO)_2Ca$ are the most common Ca^{+2} sources, while H_3PO_4, $NH_4H_2PO_4$, $(NH_4)_2HPO_4$, Na_3PO_4, and K_3PO_4 are the most common phosphorus sources (Nazarian et al., 2008). The pH of the solution is adjusted with ammonia gas, NH_4OH, or NaOH. Characteristically, in the initial stage of the process, the precipitate differs in composition from HA. Storage of the calcium phosphate precipitate under appropriate conditions increases the Ca:P ratio and leads to HA crystallization. The rate of this process depends on many factors, including the concentrations of the starting salts, mixing sequence and rate, solution pH, reaction temperature, and holding time. Because of this, control over all synthesis conditions is critical for obtaining reproducible results (Rezwan et al., 2006 , Lu et al., 2003).

Highly crystalline hydroxyapatite powder was prepared by the co-precipitation method in ethanol-water medium keeping a 1:1 M ratio. Firstly, the solution of Calcium hydroxide ($Ca(OH)_2$Loba Chemicals,≥98% purity) was stirred for 15 min. Further, the solution of Di-ammonium hydrogen orthophosphate ($(NH_4)_2HPO_4$, Loba Chemicals, ≥97% purity)was added keeping the Ca/P ratio to 1.67 and stirred for another 15 min pH of the solution was kept at 9 by adding 0.1 N NaOH (Loba Chemicals, ≥99% purity) solution. The solution was further stirred for another 60 min. The solution was filtered and washed several times. The precipitate was dried in an oven at 60°C for 24hr. The dried powder was sintered at 1000°C for 6 h.

3.2.3 Calcium Zirconium Silicate (Baghdadite) bio ceramic

For baghdadite synthesis, a solid-state method was used. Calcium carbonate ($CaCO_3$), zirconium oxide (ZrO_2), and quartz (SiO_2) were taken as raw materials. Raw materials were mixed in an appropriate weight to maintain the molar ratio of calcium oxide: zirconium oxide: silica in 3:1:2. For composite preparation, zinc oxide powder was used to partially substitute calcium with 0.1, 0.25, and 0.5 mol%. Powder sintered at 1400, 1350, and 1300°C for 3 h with constant heating and cooling rate of 2°/min. All reagents purchased from Loba Chemicals with a min 98% assay.

3.2.4 Zinc Oxide

In this work, Zinc oxide was used in as received form (Loba Chemicals,≥98% purity).

3.2 Composite preparation

Table 3.2 Bioactive glass hydroxyapatite composite system.

Sample Code	Hydroxyapatite (wt. %)	Bioactive glass (wt. %)
BG_H0	0	100
BG_H20	20	80
BG_H50	50	50
BG_H80	80	20

Table 3.3 Baghdadite Zinc Oxide composite system.

Sample Code	ZnO (mol %)
CaZn0	0
CaZn0.1	0.1
CaZn0.25	0.25
CaZn0.5	0.5

Table 3.4 Bioactive glass Zinc Oxide composite system

Sample Code	Zinc Oxide (wt. %)	Bioactive glass (wt. %)
BZn0	0	100
BZn2	2	98
BZn4	4	96
BZn5	5	95

Table 3.5 Bioactive glass baghdadite composite system

Sample Code	Baghdadite (wt. %)	Bioactive glass (wt. %)
BG	0	100
BG20	80	20
BG50	50	50
BG80	20	80

3.2.1 Granulation and pellet processing

The obtained powder after calculation was uniformaly mixed using a pestle in an agate mortar. Afterwards, 2% polyvinyl alcohol (PVA) was uniformly mixed into powder until it becomes fine. The obtained fine powder was then pelletized using a hydraulic press with the help of a die having 10 mm diameter by applying the pressure. The obtained pellets are then used for further characterization.

3.3.2 Sintering

Sintering is the heating process for microstructural change, densification, and crystal growth of the material. Sintering of the materials has been carried out in several steps of thermal heating. The furnace was heated to 500ºC at a heating rate of 2ºC /min, kept at this temperature for 2 h to burn off the binder completely. Then pellets were further heated to the required temperature at a heating rate of 2ºC /min and hold for this temperature. The pellets were then cooled to room temperature at a rate of 2ºC /min. The further characterization techniques to study the phase formation, microstructure, and mechanical properties of pellets were carried out and described in the subsequent section.

3.3 Materials Characterization techniques

The following sections describe the relevant techniques used to characterize the samples. The basic principles behind each of the techniques will be briefly described with any relevant additional information included in the appendices.

3.4.1 Thermal analysis (TGA-DSC)

The simultaneous TGA/DSC instrument has a sample head that contains two alumina crucibles one for sample holding and the other one for reference. The sample is heated

according to a predetermined temperature profile. The variation in mass is measured as a function of temperature, while the temperature difference between the sample and the reference material is measured simultaneously. During the experiment, the reference substance does not change its thermal properties or interfere with the testing gas. If there is a temperature differential between the sample and the reference, that is due to a variation in the sample's physical properties. An exothermic reaction is associated with crystallization, whereas an endothermic reaction is associated with freezing.

The thermo-gravimetric analysis (TGA) is a technique that is used to determine the calcination temperature of the sample and also used to evaluate the stability of materials. In this analysis, the change in mass of the experimental sample has been recorded as a function of temperature which provides information about the mass gain (absorption), mass loss (desorption), phase transition, etc. of the sample (Cammenga et al., 1995). If the mass of the sample remains constant in a given temperature range, then the sample is said to be thermally stable within that temperature range. TGA also provides information about the upper limit of temperature beyond which the sample starts degrading. In literature, TGA is widely used to know about the reaction temperature of the sample, stability of materials, etc. Differential scanning calorimetry (DSC), measures the change of the difference in the heat-flow rate of the sample to the reference sample when subjected to a controlled temperature program. The sample of known mass is heated or cooled during the process; the change in heat capacity is recorded in terms of changes in heat flow. Using this technique, the type of reaction (Endothermic or Exothermic), enthalpy, Gibbs energy, and other thermal parameters are derived. The combined study of TGA/DSC also gives an idea about the reaction pathway for the prepared mixture of raw materials and various transition points such as melting point, glass transition temperature, crystallization temperature, etc(Huang et al., 2016). In the present thesis work, the TGA/DSC measurement was carried out by the TGA/DSC (Mettler

Toledo, Germany) model, operated within the temperature range from 27ºC-1000ºC in the presence of nitrogen gas atmosphere.

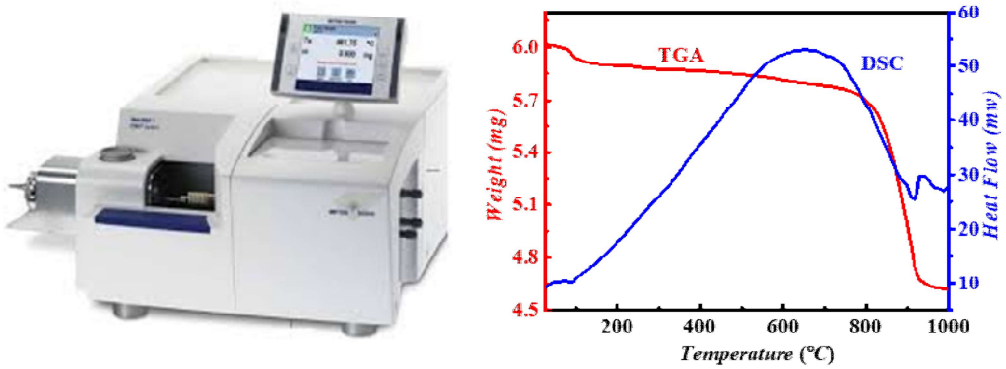

Figure 3.1 DSC-TGA instrument.

3.4.2 Phase Formation and Crystal Structure Studies by XRD

The powder X-ray diffraction (XRD) is a versatile and an essential characterization technique for phase identification which has been established over the years. The name powder X-ray diffraction is associated with the technique which connects XRD pattern from a packed powder specimen. The powder samples are made up of many microscopic polycrystals, randomly oriented domains in all possible directions, resulting in the XRD pattern. The domain which gives diffraction in the same direction is known as coherently diffracting domains. This technique is used to determine the crystal structure, preferred orientation of lattice planes, crystallite size, and shape and size distribution of polycrystalline powder (Prabhu et al., 2014). It is a non-destructive technique in which the samples can also be exposed to different pressure and temperature conditions during collection of the diffraction pattern. It is technique used to determine the crystalline phases of a material using monochromatic X-rays. When a wave interacts with a uniformly spaced lattice with a spacing

of equal size to the wavelength of the X-rays, diffraction occurs. X-rays are used when investigating crystallographic structures due to the wavelength of an X-ray being similar to the atomic spacing of many materials; this allows diffraction to occur forming constructive and deconstructive interference of the X-rays. This can be described schematically by **Figure 3.2.**

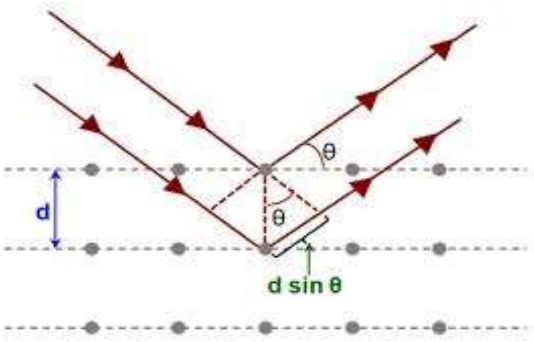

Figure 3.2 Visualization of Bragg's law.

The basic geometry used in most of the X-ray diffractometer is shown in **Figure 3.3**.

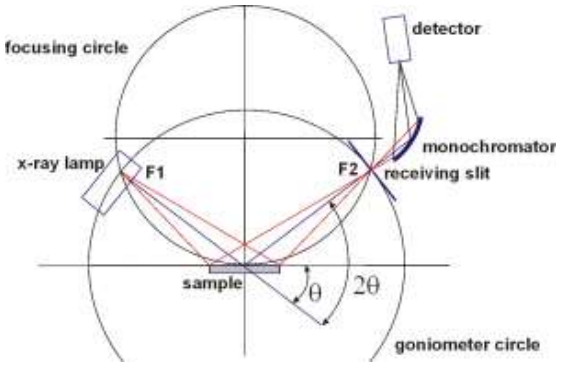

Figure 3.3 Schematic representation of $\boldsymbol{\theta/2\theta}$ diffraction in Bragg-Brentano geometry.

The XRD data were recorded in step scan mode with a slow scanning rate. The different crystallographic phases of the present sample were extracted by recording X-ray diffraction pattern at room temperature using, X-ray diffractometer (Rigaku Miniflex II, Japan) equipped with Cu Kα radiation having wavelength λ=1.5418 Å at an applied voltage of 40 kV and current 40 mA. The XRD pattern has been recorded in the angular range of 20°-80° with step size 0.02° and scan at 0.02°/min. We have used the width of the primary divergence slit was 0.6 mm, and for the secondary detector, the slit was at 1.0 mm for X-ray diffraction measurements. The X-ray diffractometer used for present thesis work is shown in **Figure 3.4**. For this experiment, composite samples had to first be prepared, modified, and then crushed and ground into a fine powder before performing XRD characterization.

Figure 3.4 XRD instrument, Central Instrument Facility (CIF, IIT BHU).

3.4.3 Fourier Transform Infrared Spectroscopy (FTIR)

Infrared spectroscopy is an important technique for the analysis of materials also provides the fingerprint of the samples investigating in this work. The absorption of FTIR peaks corresponding to the frequencies of vibrations between the bonds of the atom which is responsible for building up the materials. Since each material possesses a unique combination of atoms and no two compounds produce the exactly same infrared spectrum. Thus IR spectroscopy can provide identification (qualitative analysis) of different kinds of materials (Titus et al., 2019). A schematic diagram of Fourier transforms infrared (FTIR) spectroscopy

is shown in **Figure 3.5**. The FTIR is preferred over other infrared spectrum analysis due to following reasons

- It is a non-destructive technique.
- It provides a precise measurement method which requires no external calibration.
- It can increase the speed of data collection and scan every second.
- It has greater optical throughput.
- It is mechanically simple with only one moving part.

In FTIR, a beam of light of different frequencies interacts with the sample, which excites and vibrates the covalent bonds containing dipole moments, and the detector detects the intensity of light after the interaction. To determine the amount of light absorbed at each wavelength, the interferogram is subjected to a Fourier transform. The data set can be collected in reflected, absorbed, or transmitted mode. The energy consumed by the bonds is determined by the type of bonds present resulting in a characteristics spectrum (Berthomieu et al., 2009). The composites in this work were analyzed using FTIR before and after immersion in SBF for bioactivity analysis to see whether any modifications had occurred. All samples were ground into a fine powder, and spectra were determined at a resolution of $2cm^{-1}$ ranging from 400 to 4000 cm^{-1}. Data were collected in transmission mode using an FTIR (BRUKER, TENSOR 27) operating in attenuated total reflectance (ATR) mode as shown in **Figure 3.5.**

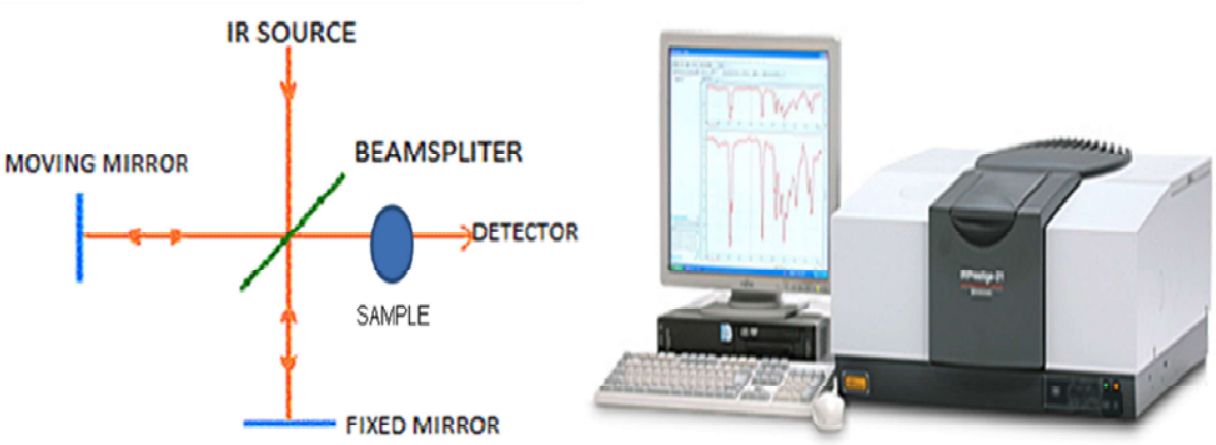

Figure 3.5 Principle of FT-IR spectroscopy and experimental set-up for FTIR measurement facility.

3.4.4 Microstructure and Elemental Analysis.

3.4.4.1 Field Emission Scanning Electron Microscope (FESEM)

A field emission cathode in electron gun of a scanning electron microscope provides a narrower beam at low as well as high electron energy, resulting in both improved spatial resolution and minimized sample charging and damage (Goldstein et al., 2017). The electrons were generated by a field gradient in the presence of vacuum, then the beam passes through electromagnetic lenses was focused onto the specimen which results generation of various types of electrons through this interaction. A detector ascertained the secondary electron and an image of the surface sample are formed by comparing the intensities of secondary electrons to the primary electron beam. Finally, the image is displayed on monitor equipped with the FESEM. The FE-SEM images of the investigated samples in this thesis work have been recorded by EVO18, Zeiss, Japan as shown in **Figure 3.6**.

Figure 3.6 FESEM facilities, IIT (BHU).

3.4.4.2 Energy dispersive X-ray spectroscopy (EDX)

The non-destructive Energy Dispersive X-ray analysis commonly known as EDX or Energy dispersive spectroscopy analysis (EDS) is an X-ray analysis to identify the elemental composition of materials of 0.5 to 1 atomic percent sensitivity. This facility is generally attached with electron microscopy instrument (SEM, TEM) where a specimen of interest is identified by the impact of a high energy electron beam and ejected electrons from inner shell of atomic orbitals of elements present in the sample. The resulting vacancy of the inner shell is filled by the electrons available in shell close to the vacant shell; these transitions are emitted as X-rays. Thus the information corresponding to the elements of the samples can be analyzed on the basis of energy of emitted X-ray. EDX gave qualitative, semi-quantitative information about the elements present in the composition. In the present thesis work, the elemental compositions of the prepared samples were confirmed from energy-dispersive X-ray analysis using EDXA spectrometer as shown in **Figure 3.6** attached with FESEM/ EVO18, Zeiss, Japan. This technique was primarily used to detect the elements present in the tested samples and to examine the change in composition of the composites surfaces after the samples were immersed in SBF.

3.4 In vitro bioactivity studies

The bioactivity of any biomaterials is determined by immersing the biomaterials in simulated body fluid (SBF). The formation of hydroxyapatite over the surface is the main criteria to measure the bioactivity. The preparation of SBF was tailored specifically to obtain the ionic concentrations listed in **Table 3.6** which closely resembled the ionic concentration of blood plasma.

Table 3.6 Ionic composition of SBF compared to human blood plasma (Kokubo et al., 2006).

Ion	Simulated body fluid (SBF) Concentration (mmol/L)	Human blood plasma Concentration (mmol/L)
Na^+	142.0	142.0
K^+	5.0	5.0
Mg^{+2}	1.5	1.5
Ca^{+2}	2.5	2.5
Cl^-	147.8	103.0
HCO_3^-	4.2	27.0
HPO_4^{-2}	1.0	1.0
SO_4^{-2}	0.5	0.5

SBF is prepared according to the standard procedure discovered by Kokubo et al., 2006 by dissolving a range of chemicals as shown in **Table 3.7**. For the preparation of 1000 mL SBF, firstly, a thoroughly cleaned polyethylene beaker was filled with 750ml of deionized water and stirred at 37°C. Next, the chemicals were added one at a time in the order shown in **Table 3.7.** Each chemical was left to stir until completely dissolved before the subsequent chemical was added. The tris-buffer $[(CH_2OH)_3CNH_2]$ was added carefully to prevent the

sudden rise in pH of the solution. The pH of the final solution was adjusted to pH 7.40 using 1M HCl at 37°C. Afterthat, the solution was made up to 1000 mL with deionized water and cooled to room temperature before being stored in a refrigerator. In this experiment, powders were soaked in SBF solution for 3, 5, 7, 14, 21 and 28 days in an incubator at 37°C. The ratio of SBF to powder was kept 100:1. After a defined soaking period, powders were removed from the solution and the pH of the solution was measured. After this, wet powders were dried and apatite layer formation over the sample surface was characterized by XRD, FTIR, and SEM techniques.

Table 3.7 Chemicals used for the preparation of simulated body fluid (SBF)

S.No.	Chemical	Quantity
1	NaCl	7.996g
2	$NaHCO_3$	0.350g
3	KCL	0.224g
4	$K_2HPO_4.3H_2O$	0.228g
5	$MgCl_2.6H_2O$	0.305g
6	HCL	$40cm^3$ with a concentration of $1kmol/m^3$
7	$CaCl_2$	0.278g
8	$NaSO_4$	0.071g
9	$(CH_2OH)CNH_2$	6.057g
10	HCL	as much as is required to change the pH with a concentration of 1kmol/m3.

3.5 Degradation analysis

To determine the degradation of composite materials, equally sized cylindrical pallets of 10 mm radius and 2.0 mm in height were immersed in SBF and incubated at 37ºC for defined days. After desired time period, the samples were removed, wiped, and dried at 60°C for overnight. Changes in the weight of the composites after immersion in SBF were weighted. The degradation in terms of weight loss and water absorption was calculated by the following equations (3.1) and (3.2).

$$Weight\ loss \quad \%WL = \frac{W_{0\ dry} - W_{t\ dry}}{W_{0\ dry}} \times 100 \qquad (3.1)$$

$$Water\ absorption\ \%WA = \frac{W_{t\ wet} - W_{t\ dry}}{W_{0\ dry}} \times 100 \qquad (3.2)$$

Where, $W_{0,\ dry}$ is the original sample weight taken before immersion in SBF.

To measure the water absorption (%*W*A) immersed samples were removed at given time period, gently wiped, and weighed ($W_{t,\ wet}$). Similarly, to measure the weight loss (%*W*L) the samples were removed from the SBF solution, dried at 37°C overnight, and subsequently weighed ($W_{t,\ dry}$).

3.6 Determination of Compressive Strength

A Compression test was conducted to determine the stress and strain of all composites. Stress is defined as the instantaneous load applied to a specimen divided by its cross-sectional area (Roeder, 2013). Using compression test, the sample is deformed along the direction of the applied stress; as such the output recorded will be the force applied against the change in sample length. Three samples of each composition were used to measure the compressive strength. The obtained results were averaged. Composite samples were prepared into pallets of size 10*5 mm^2 into cylinders before sintering. Polished samples

were prepared in such a way that all sides were crack-free, and parallel. The samples were compressed on Tinius Olsen H10KL UTM at a crosshead speed of 0.5 mm/min. The stress was calculated using equation (3.3).

$$compressive\ stress\ \sigma = \frac{Force}{Cross\ sectional\ area} \qquad (3.3)$$

3.7 Measurement of Density

The density (ρ) of prepared composites was calculated using the Archimedes principle. For this purpose, the pellets of each composition were made. The powders of each composition were mixed with 2% polyvinyl alcohol (PVA) and pelletized with the help of a vertical die having diameter of 10 mm and thickness of 2 mm by Hydraulic press. In this method, firstly pellets were weighed in air, later on; the pellets were immersed into the water. Let w_a and w_w was the weight of pellet in air and water respectively, and the density of the sample was calculated by following equation. (3.4)

$$\rho = \frac{W_a}{w_a - w_w} \times \rho_w \qquad (3.4)$$

Where, ρ_w is the density of water.

The theoretical density (ρ_{glass}) of bioactive glass can be calculated from the following expression:

$$\rho_{glass} = (xSiO_2 * dSiO_2 + xCaO * dCaO + xNa_2O * dNa_2O + xK_2O * dK_2O + xMgO * dMgO + xP_2O_5 * dP_2O_5 + xZrO_2 * dZrO_2) \qquad (3.5)$$

Where, x is the molar fraction and d is theoretical density value in kg/m^3, respectively (Helmy et al., 2018).

The composite density (ρ_0) measured by rule of mixture is obtained by given equation.

$$\rho_{0=\frac{1}{\frac{w_r}{\rho_r}+\frac{w_m}{\rho_m}}} \qquad (3.6)$$

Where $w_r$the weight fraction for reinforcement material, w_m is is the weight fraction for matrix, ρ_r is the density of reinforcement material and, ρ_m is the density of matrix. The density of baghdadite is 3.48*10^3 kg/m^3 and the density of bioglass is calculated by equation (3.5).

In the present thesis work, three different pellets of each composition were weighed three times and their average value is taken as the experimental density of the sample. The weighing measurement was performed using a digital balance having an accuracy of ±0.0001 gm. as shown in **Figure 3.7**.

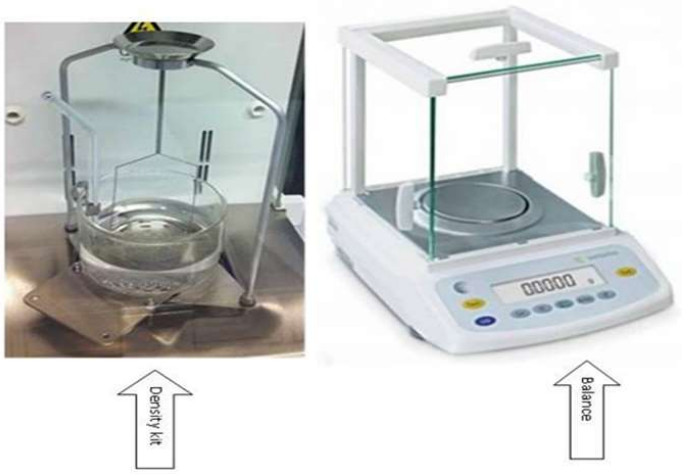

Figure 3.7 Balance with density kit [Sartorius, BSA2245CW**]**.

3.8 Biological Evaluation

Osteoblasts are responsible for bone formation, more specifically for the mineralization of the osteoid matrix. In this work, the MG 63 cell line was cultured on the composites in order to evaluate how the produced networks would behave when in contact

with tissues. Hard (human osteoblasts-like) tissue models were considered to be an important evaluation of the tested materials.

3.8.1 Cell culture

MG-63 cell line was obtained from NCCS Pune, India. The cell line was maintained in Dulbecco's Modified Eagle's Medium (DMEM) supplemented with 10% Fetal Bovine Serum (FBS), 1% Penicillin/Streptomycin antibiotic at 37°C in a 5% CO_2 humidified incubator. Cell proliferation within the composite was assayed by MTT (3-[4,5-dimethyl-thiazol-2-yl]-2,5-diphenyltetrazolium bromide) assay. This assay is based on the principle that metabolically active cells reduce yellow color tetrazolium MTT into intracellular purple formazan through dehydrogenase enzyme activity. This purple color formazan was quantified via the spectrophotometric method after solubilization with DMSO. The rate of cell proliferation is reciprocal to the rate of tetrazolium reduction. Cell viability was calculated by the following equations

$$Cell\ viability_{sample}\ \% = \frac{Ab_{sample}}{Ab_{control\ 7\ day}} \times 100 \qquad (3.7)$$

$$Cell\ viability_{control}\ \% = \frac{Ab_{control}}{Ab_{control\ 7\ day}} \times 100 \qquad (3.8)$$

For this experiment, MG-63 cells were seeded on each composite sample at a density of 10^4 cells/mL and incubated for 1 h in a 5% CO_2 incubator for cellular adhesion. To reduce the chances of false reading/result due to the cells that were migrated and adhered to on the surface of Petri plates, the composite sample was transferred into 96-well plates for prolonged culture. Cells seeded samples were then maintained in a 5% CO_2 incubator for 2, and 7 days. Cells cultured without any composite in the wells were considered as a positive control and a complete growth medium was used as a negative control for all the experiments. After incubation, the culture medium was removed from each well, and

composites were transferred again into new fresh wells to avoid the chances of false reading due to the cells that were migrated and adhered to the bottom of the well during incubation. A total of 100 µL MTT solution comprising of a complete growth medium (DMEM + 10% FBS + 1% PS, 90 µL) and MTT (5 mg/mL in PBS, 10 µL) was added to each well. After 4 h of incubation, the formazan crystals formed inside the wells were solubilized using a 100 µL dimethyl sulfoxide (DMSO) solution for 15 min. After pipette-mixing, the solution mixture was transferred to the fresh wells to avoid the absorbance arising due to the scaffold. The optical absorbance was measured at 570 nm on a multimode microplate absorbance reader (Synergy H1 hybrid, Biotek, USA). MTT assay was performed in triplicates for both cell lines along with positive controls (Varshney et al., 2019).

In the experiment, the rate of cell proliferation (viability) within the composites has been investigated using an MTT assay. The percentage of cell viability within the composite was calculated for the absorbance of positive control observed on day 7.

3.8.2 Nuclear staining

To visualize the cell distribution within the composite, the nuclei were stained with 4,6- diamidino-2-phenylindole (DAPI) (1 µg/mL), which is a fluorescent stain that binds to A-T rich region of DNA and fluoresces blue upon excitation at a wavelength of 358 nm. Culture medium was removed from the Petri dish containing the composite embedded with the cells. The composite was then washed thrice with 1×PBS to remove leftover media and debris content. Cells within the composite were fixed by adding 100 µL of 4% paraformaldehyde for 15 min at room temperature followed by washing with PBS (1×) to completely remove unbound paraformaldehyde. After fixation, the cells were permeabilized for dye infusion by adding 100 µL of 0.1% (v/v) Triton X-100. After incubation for 5 min, scaffolds were washed thrice with 1× PBS to prevent high degradation of the cell membrane. To block the nonspecific binding of stain, 100 µL of 1% bovine serum albumin (BSA)

solution was added post-PBS washing. Unbound BSA was removed by washing with PBS thrice followed by staining of the cells embedded within the composites with DAPI (1 μg/mL) and incubation for 30 min in a dark room to prevent stain bleaching. 50μL glycerol (80%) was added to the composite to prevent cells from dehydration and finally observed under a fluorescent microscope (Varshney et al., 2019).

3.9 Hemocompatibility

The hemolytic activity of composite measured according to the method described as ASTM F 756-00 (ASTM, 2000). For this, each powder sample was added in 7 ml of PBS and incubated at 37°C for 72 h. After removing PBS solution from the sample solution, the 1 ml diluted blood (9.02 mg/mL) of acid citrate dextrose (ACD) rat venous was added to each sample and incubated for 3 h at 37°C. After that, the solution centrifuged at 2000 rpm for 15 min. The ACD blood solution with distilled water designated as positive while the ACD blood solution with PBS marked as a negative control. The hemoglobin amount was analyzed by hemolysis activity and determined by measuring the optical densities (O.D.) at 540 nm using a Micro-plate Reader (Synergy HT Multi-Mode, BioTek, USA). For error minimization, triplicates of each sample were taken to average their optical density values. The hemolysis rate (%) was calculated by equation (5) (Hossain et al., 2020).

The obtained results are compared with the ASTM standard. The composites are assigned as non-hemolytic for <5% hemolysis rate and hemolytic for > 20 % hemolysis rate (Ali et al., 2018).

$$\%\ \text{Hemolysis control} = \frac{\text{O.D.of a sample} - \text{O.D.of negative control}}{\text{O.D.of positive control} - \text{O.D.of negative control}} \times 100 \qquad (3.9)$$

3.103.9 Anti-Bacterial Evaluation

MTT assay was used to measure the viability of *E. coli* and *S. aureus* bacterial cells on the composite samples. The samples were seeded with 150 µL of 0.1 OD bacterial cultures in 350 µL of respective media and incubated for 10 h at 37°C. After incubation, the culture was removed from the samples which were followed by washing with 1x phosphate buffer saline (PBS) to remove media debris and dead bacterial cells. Afterwards, 500 µL of reconstituted MTT (MTT: 1x PBS as 1: 10) was added in each well (24 well tissue culture plate) and further incubated for 2 h at 37°C to allow for the formation of formazan crystals. Now, MTT from each sample was replaced by dimethyl sulfoxide (DMSO) to dissolve formazan crystals and the OD of these dissolved formazan crystals were measured using ELISA microplate reader (Bio-red) at 595 nm, which represents the viability of bacterial cells (Khare et al., 2021).

$$Bacterial\ viability\ (\%) = {}^{O.D.of\ sample}/_{O.D.of\ Blank} \times 100 \quad (3.10)$$